

Azomethine ylide-formation from *N*-phthaloylglycine by photoinduced decarboxylation: A theoretical study

FANG Qiu, DING LiNa & FANG WeiHai*

College of Chemistry, Beijing Normal University, Beijing 100875, China

Received May 30, 2012; accepted June 18, 2012; published online August 21, 2012

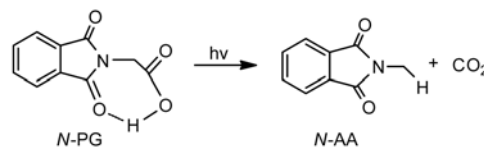
In this work, we report the first CASPT2//CASSCF study of the mechanism of the photodecarboxylation of *N*-phthaloylglycine. The charge transfer excited state $S_{CT}(^1\pi\pi^*)$ is initially populated upon irradiation at 266 nm. As a result of a fast internal conversion to the lowest excited singlet state $S_{CT-N}(^1\pi\pi^*)$, this state becomes a favorable precursor state for proton transfer, which triggers decarboxylation. Actually, the excited state intramolecular proton transfer (ESIPT) and decarboxylation processes proceed in an asynchronous concerted way. The ESIPT process is accomplished in the $S_{CT-N}(^1\pi\pi^*)$ state, but the CO_2 molecule is finally formed in the ground state via the S_{CT}/S_0 conical intersection. Azomethine ylide is formed in the ground state as a complex with CO_2 . A barrier of ~15 kcal/mol indicates that azomethine ylide is stable in the ground state, which is consistent with the experimental findings. This work provides mechanistic details about the formation of azomethine ylide by photoreaction of *N*-phthaloylglycine.

***N*-phthaloylglycine, photodecarboxylation, excited state intramolecular proton transfer, CASPT2//CASSCF method**

1 Introduction

The primary α -photodecarboxylation of *N*-phthalimido-amino acids and the subsequent reactions with dipolarophiles have been extensively investigated over the past three decades [1–10]. The reason for this is that the 1,3-dipolar cycloaddition reaction of azomethine ylides with dipolarophiles is an efficient and versatile method for the construction of five-membered heterocycles, especially, the use of alkenes as dipolarophiles for the synthesis of pyrrolidine-containing molecules of biological or materials science interest. As the simplest *N*-phthalimido-amino acid, *N*-phthaloylglycine (*N*-PG) can generate *N*-alkylphthalimide (*N*-AA) when irradiated in organic solvents, which undergoes clean and efficient α -photodecarboxylation. This process is summarized in Scheme 1.

In earlier investigations, laser flash photolysis and fluorescence spectroscopy have been employed to investigate



Scheme 1 Photo-induced decarboxylation of *N*-phthaloylglycine.

the mechanistic details of the α -photodecarboxylation and related excited state processes. The results of the previous work suggest that azomethine ylides are the key reactive intermediates in these processes. In addition, the investigations provided information about the dynamics of several ylide decay pathways and the nature of the excited states responsible for the ylide formation and decarboxylation reactions. An excited state proton transfer (ESPT) mechanism was postulated for the decarboxylation reaction in early experimental studies [1–5], and this is coupled with electron transfer leading to the *N*-AA product. The mechanistic studies by Yoon and co-workers suggested that this α -photodecarboxylation process was initiated by hydrogen

*Corresponding author (email: Fangwh@bnu.edu.cn)

atom abstraction and further proceeds via an azomethine ylide intermediate resulting in formation of the *N*-AA product [4–9]. The intramolecular H-bond formation in the ground and excited states of *N*-phthaloylglycine (*N*-PG), which facilitates proton transfer, was evidenced by X-ray structure analysis, cyclic voltammetry, and IR spectroscopic measurements in photoinduced-electron-transfer-active phthalimido carboxylic acids [11], together with a significant enhancement of fluorescence efficiencies [10, 12, 13], but with very weak fluorescence of the phthalimide chromophore itself [12–17]. Meantime, the azomethine ylide intermediate was trapped by cycloaddition with carbonyl or alkene dipolarophiles. In addition, the azomethine ylide intermediate was characterized by observation of a 392-nm-absorbing transient in laser flash photolysis studies [4–6]. However, how azomethine ylides are produced upon irradiation of *N*-phthalimido-amino acids in organic solvents, which is the key issue, remains unsolved up to now.

The phthalimide group is a very useful chromophore and shows the typical reactivity of excited state carbonyl chromophores. In addition, the phthalimide chromophore is characterized by a high oxidation potential of its first excited singlet state and excited triplet states. The ylide formation photoreactions are an appealing route in synthetic organic photochemistry because they can serve as the foundation for preparing interestingly structured and functionalized *N*-heterocyclic products [8, 9]. Because of the versatile photochemical reactivity of phthalimides and their applicability in synthesis, the photochemistry of phthalimides is still a subject of widespread interest.

The photophysical properties of phthalimides have been intensively studied during the last two decades [6–9]. Phthalimides show relatively unstructured UV absorption spectra with absorption maxima around 220 and 295 nm. In ethanol or acetonitrile at room temperature, *N*-alkylphthalimides exhibit weak fluorescence with low quantum yields. The fluorescence properties are sensitive to solvent polarity and, in protic solvents, also to hydrogen bonding. In general, phthalimides show a broad structureless phosphorescence centered around 450 nm with a long triplet lifetime at room temperature in the absence of oxygen. However, the order of the excited states for phthalimides remains controversial. In addition, there is a general lack of the information about the excited state nature responsible for ylide formation from *N*-PG [10–17].

In this work, we report the first theoretical study of the nature of the excited state that is responsible for the ylide formation by using combined complete-active-space self-consistent-field (CASSCF) and multireference perturbation treatment to the second order (CASPT2) methods with *N*-PG as a representative molecule. The decarboxylation process was found to be triggered by a proton transfer in the lower singlet excited state $S_{CT-N}({}^1\pi\pi^*)$ which was reached via charge redistribution from the bright charge transfer

singlet excited state $S_{CT}({}^1\pi\pi^*)$. The conical intersection of $S_{CT}({}^1\pi\pi^*)/S_0$ is an efficient decay channel to the ground state with ylide character and has a suitable orientation for reverse proton transfer. Subsequent electron transfer and proton transfer in the ground state lead to the final products.

2 Computational details

The CASSCF wave function has sufficient flexibility to model the changes in electronic structure upon electronic excitation, and was used to optimize the stationary structures of *N*-PG in several low-lying electronic states. The conical intersection structure was determined by the state-averaged CASSCF method. To consider dynamical correlation, the single-point energy was calculated with the second-order perturbation method (CASPT2) on the basis of the CASSCF reference wave function. The CASPT2 energies were calculated using five-root state-averaging with equal weights. The 6-31G* basis set was used for both CASSCF and CASPT2 calculations. All calculations were performed by using Molcas 7.1 [18] and Gaussian 03 [19] program packages.

In principle, all of the valence electrons and orbitals of a system should be included in the active space for the CASSCF calculations. However, because of the limited computational capability, the complete active space formalism contains a certain amount of ambiguity in terms of which particular electrons and orbitals are chosen for inclusion in practice. For this reason, selection of the active space becomes a crucial step in CASSCF calculations. In this study, to describe the reaction of proton transfer, O–H σ and σ^* orbitals and the oxygen non-bonding orbital of the carbonyl group should be included in the active space. Since electronic excitation from the aromatic ring to the acetyl group is involved in the charge transfer (CT) state, at least the aromatic π and acetyl π^* orbitals are very important for the CT state. The five relevant orbitals are shown in Figure 1.

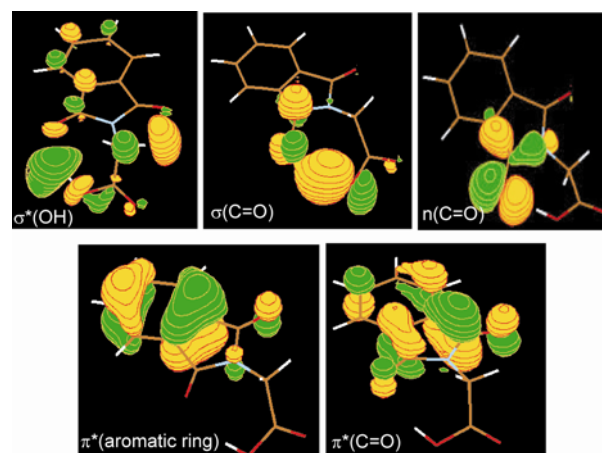


Figure 1 Selected active orbitals that are closely related to charge transfer in the excited state and proton transfer.

In order to treat electronic correlation well, some π and π^* orbitals were also included in the active space. Finally, the CASSCF and CASPT2 calculations were performed with an active space of 14 electrons in 11 orbitals, referred to as CAS(14,11) hereafter.

3 Results and discussion

3.1 Low-lying electronic states

Electronic and geometric structures of excited states are basic, but very important, parameters for photochemical and photophysical processes. Before discussing the photodecarboxylation, we pay attention to excited state nature of *N*-PG. Besides the ground state (S_0), the three low-lying singlet excited states were optimized at the CAS(14,11)/6-31G* level. The resulting structures are shown in Figure 2, where the key bond parameters are given with the atom numbering in the S_0 structure. The first excited singlet state in the Franck–Condon (FC) region was found to originate from an electronic transition from $n_{(C=O)}$ to $\pi^*_{(C=O)}$ and is the ${}^1n\pi^*$ state, referred to as $S_{CO}({}^1n\pi^*)$ hereafter. As a result of the $n_{(C=O)} \rightarrow \pi^*_{(C=O)}$ transition, the C15–O14 bond length is significantly increased on going from S_0 to $S_{CO}({}^1n\pi^*)$. The second excited singlet state in the FC region comes from the local excitation at the phenyl ring and is assigned as the $\pi\pi^*$ singlet state of $S_{Ph}({}^1\pi\pi^*)$. In comparison with the S_0 structure, the C–C bond lengths are elongated by about 0.3 Å in the $S_{Ph}({}^1\pi\pi^*)$ structure.

A high-energy excited singlet state in the FC region, referred to as $S_{CT-N}(^1\pi\pi^*)$, was found to involve a transition from the π orbital of the aromatic ring to the π^* orbital of the carbonyl group, which is of charge transfer character.

When the system relaxes to the $S_{CT-N}({}^1\pi\pi^*)$ minimum energy structure, charge is redistributed through the π conjugation system. The CAS(14,11)/6-31G* calculations show that the Mulliken charges on the N8 and O14 atoms are -0.91 and -0.52 respectively in the S_0 equilibrium structure, while they become -0.42 and -0.75 in the $S_{CT-N}({}^1\pi\pi^*)$ structure. The $\pi_{(\text{aromatic ring})} \rightarrow \pi^*_{(C=O)}$ transition and the subsequent charge redistribution are summarized in Figure 3. The larger amount of negative charge localized on the O14 atom suggests that proton transfer takes place easily in the $S_{CT-N}({}^1\pi\pi^*)$ state. This is consistent with the optimized $S_{CT-N}({}^1\pi\pi^*)$ structure, where the O14 \cdots H13 hydrogen bond is much shorter than that in the S_0 structure.

With respect to the S_0 zero-level, the relative energies of $S_{CO}(^1n\pi^*)$, $S_{Ph}(^1\pi\pi^*)$, and $S_{CT-N}(^1\pi\pi^*)$ were calculated at the CASPT2 level on the CAS(14,11) optimized structures. The adiabatic excitation energies (ΔE_{adia}) from S_0 to $S_{CO}(^1n\pi^*)$, $S_{Ph}(^1\pi\pi^*)$, and $S_{CT-N}(^1\pi\pi^*)$ were predicted to be 90.3, 92.9, and 82.4 kcal/mol, respectively. $S_{CT-N}(^1\pi\pi^*)$ becomes the lowest excited singlet state in view of its adiabatic excitation energy, although the $S_{CT-N}(^1\pi\pi^*)$ state is high in energy in the FC region, as can be seen from the CASPT2 calculated energies listed in Table 1. It should be pointed out that

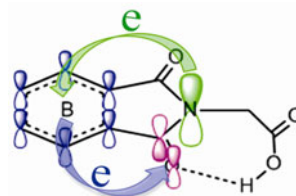


Figure 3 Schematic electronic excitation (blue arrow) and the subsequent redistribution (green arrow) through the π conjugation system.

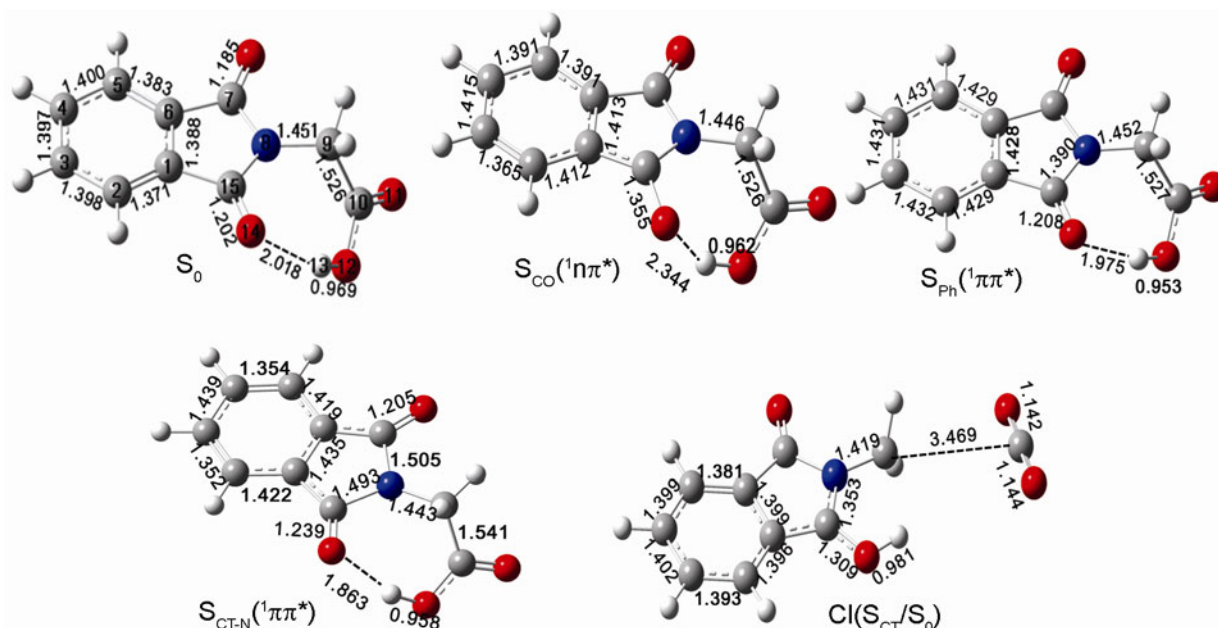


Figure 2 Schematic stationary and intersection structures along with the key bond parameters and atom numbering in the S_0 structure.

a clear charge transfer excited state of $S_{CT}(^1\pi\pi^*)$ was determined to exist in the FC region by CASPT2 calculations, which is similar to the $S_{CT-N}(^1\pi\pi^*)$ state in nature. All attempts to optimize the $S_{CT}(^1\pi\pi^*)$ minimum lead to the $S_{CT-N}(^1\pi\pi^*)$ minimum energy structure. As listed in Table 1, the $S_{CT}(^1\pi\pi^*)$ state has the largest oscillation strength and is the bright state (labeled as $S_{CT-B}(^1\pi\pi^*)$ in Figure 4).

3.2 Decarboxylation triggered by proton transfer

The decarboxylation reaction was observed to occur upon irradiation of *N*-phthaloylglycine in N_2 -saturated MeCN solution at 266 and 305 nm [10], which corresponds to the vertical excitation energies of 107.5 and 93.7 kcal/mol, respectively. It should be pointed out that our CASPT2 calculations may overestimate the relative energy of the excited singlet state, as compared with the excitation wavelength used in the experiments, since the solvent effect is not included in the calculations. Based on the CASPT2 calculated excitation energies and oscillation strengths listed in Table 2, the $S_{CT}(^1\pi\pi^*)$ state is initially populated at 266 nm. As pointed out before, the $S_{CT}(^1\pi\pi^*)$ state is unstable and relaxes to the $S_{CT-N}(^1\pi\pi^*)$ minimum very easily. It might be possible that the $S_{Ph}(^1\pi\pi^*)$ state is initially populated upon photoexcitation at 305 nm. The $S_{Ph}(^1\pi\pi^*)$ state involves a local excitation in the aromatic ring and is unreactive with respect to hydrogen or proton transfer [20, 21].

Once the $S_{CO}(^1n\pi^*)$ state is populated by photoexcitation and the subsequent relaxation, the H13 transfer from O12 to

O14 can take place easily; this is generally referred to as a Norrish type II reaction [20, 21]. The O12–H13 distance was selected as the reaction coordinate, and the potential energy profile was scanned for the H13 transfer in the $S_{CO}(^1n\pi^*)$ state. The calculated energies are listed in Table 2, which shows that the hydrogen transfer and the decarboxylation occur at the $S_{CO}(^1n\pi^*)$ state with only low probability. According to Kasha's rule [22], photochemical reactions generally occur from the lowest excited singlet state regardless of the initial excited state populated by photoexcitation. Quantitative calculations and qualitative analysis indicate that $S_{CT-N}(^1\pi\pi^*)$ functions as the most favorable precursor state for proton transfer, which will be discussed below.

The reaction pathway for the $S_{CT-N}(^1\pi\pi^*)$ state was first determined by the state-averaged CAS(14,11)/6-31G* stepwise optimization with the O12–H13 distance fixed at different values and other bond parameters relaxed fully. Then, the potential energy profile for the proton transfer and subsequent processes were characterized by the CASPT2 calculations on the basis of the CAS(14,11)/6-31G* optimized structures, as shown in Figure 4. The first observation is that the C9–C10 distance becomes remarkably elongated with the evolvement of proton transfer in the $S_{CT-N}(^1\pi\pi^*)$ state, leading to a partial breakage of the C9–C10 bond with a distance of 1.65 Å at the transition state (TS) of the proton transfer. In addition, the O11–C10–O12 angle is gradually increased to 138.4° in the TS structure. These changes in structure reveal that the decarboxylation is triggered by the excited state intramolecular proton transfer (ESIPT). Actually, the ESIPT and decarboxylation processes occur in an asynchronous concerted way. The proton is transferred from O12 to O14, which might produce a $S_{CT-N}(^1\pi\pi^*)$ -E structure. But the $S_{CT-N}(^1\pi\pi^*)$ -E minimum energy structure is not found on the $\pi\pi^*$ singlet state by the CAS(14,11)/6-31G* optimizations. With respect with the $S_{CT-N}(\pi\pi^*)$ minimum, the proton transfer reaction has a

Table 1 The CASPT2/CAS(14,11)/6-31G* calculated vertical excitation energies (ΔE_{ver} , kcal/mol), dipole moment (μ , Debye), oscillator strength (f), and adiabatic excitation energies (ΔE_{adia} , kcal/mol) for the $S_{CO}(n\pi^*)$, $S_{Ph}(\pi\pi^*)$, $S_N(\pi\pi^*)$, and $S_{CT}(\pi\pi^*)$ states

State	ΔE_{ver}	μ	f	ΔE_{adia}
S_0	0.0	7.3	—	0.0
$S_{CO}(^1n\pi^*)$	95.1	7.5	0.0	90.3
$S_{Ph}(^1\pi\pi^*)$	100.4	8.2	0.03	94.9
$S_{CT-N}(^1\pi\pi^*)$	102.9	5.8	0.01	82.4
$S_{CT}(^1\pi\pi^*)$	115.5	11.4	0.13	—

Table 2 The CASPT2/CAS(14,11)/6-31G* calculated energies and relative energies, dipole moment (μ , Debye), oscillator strength (f), and adiabatic excitation energies (ΔE_{adia} , kcal/mol) for the hydrogen transfer in the $S_{CO}(n\pi^*)$ state

H13–O12 (Å)	E (a.u.)	μ	f	ΔE (kcal/mol)
1.05	−738.70295	7.5	0.0	0.0
1.15	−738.68464	8.4	0.0	11.5
1.25	−738.66954	8.6	0.0	21.0
1.35	−738.65032	8.9	0.0	33.0
1.45	−738.63127	9.2	0.0	45.0
1.55	−738.61186	9.5	0.0	57.2
1.65	−738.60237	7.8	0.0	63.1

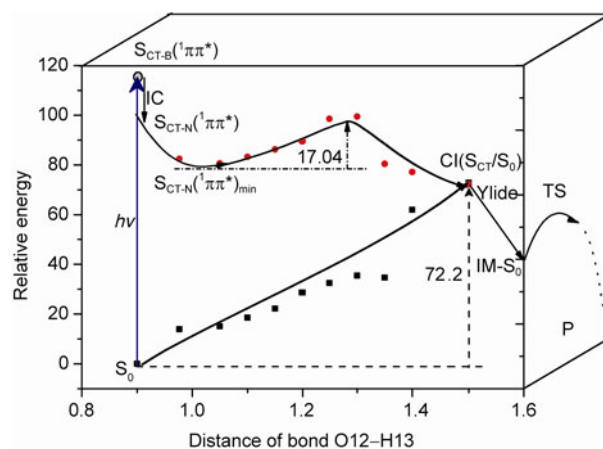


Figure 4 Schematic potential energy profiles for the proton transfer and subsequent reactions, along with the relative energies (kcal/mol) of some critical structures.

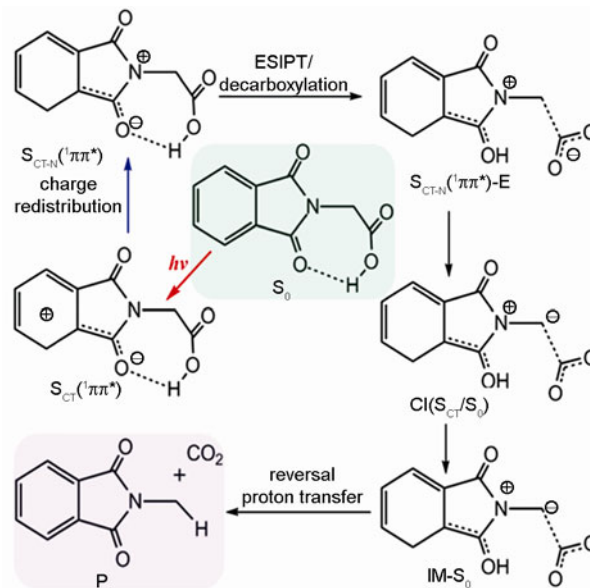
barrier of 17.0 kcal/mol at the CASPT2//CAS(14,11)/6-31G* level.

The conical intersection of the $S_{CT-N}({}^1\pi\pi^*)$ and S_0 surfaces, referred to as $CI(S_{CT}/S_0)$ hereafter, was determined using the state-averaged CAS(14,11)/6-31G* optimization. The $CI(S_{CT}/S_0)$ conical intersection was found to be 10.2 kcal/mol lower than $S_{CT-N}({}^1\pi\pi^*)$ in energy at the CASPT2//CAS(14,11) level. The C9–C10 bond is broken in the $CI(S_{CT}/S_0)$ structure with the C9–C10 distance of 3.469 Å and the O11–C10–O12 moiety of the $CI(S_{CT}/S_0)$ structure exhibiting the structural characteristics of CO_2 . There is a sharp turning point of charge translocation at the $CI(S_{CT}/S_0)$ structure. Once the system passes through the $CI(S_{CT}/S_0)$ conical intersection, electron transfer occurs from the CO_2 group to the remaining moiety. The azomethine ylide is formed in the ground state. Since a Coulomb interaction exists between azomethine ylide and CO_2 formed initially, a complex of azomethine ylide with CO_2 is obtained as the intermediate of IM- S_0 .

The isomerization pathway of the IM- S_0 intermediate to the final product (P) was traced and a transition state was determined on the S_0 pathway. The barrier height was predicted to be 15.1 kcal/mol at the CASPT2//CASSCF level. After the system decays to the ground state via the $CI(S_{CT}/S_0)$ intersection region, the system is left with sufficient internal energy to overcome the barrier, achieving reverse proton transfer in the ground state and yielding the final product. A 392-nm-absorbing transient arising from photolysis of *N*-PG was observed in the MeCN solution [4, 10], which probably comes from the azomethine ylide intermediate. The relatively high barrier (~15 kcal/mol) on the S_0 pathway from IM- S_0 to the final product indicates that the azomethine ylide is stable, which is consistent with the experimental findings.

4 Conclusions

We report the first CASPT2//CASSCF study of the mechanistic photochemistry of *N*-phthaloylglycine. Upon irradiation at 266 and 305 nm, the *N*-phthaloylglycine molecule may be initially excited to the $S_{CT}({}^1\pi\pi^*)$ state, which exhibits clear charge transfer character from the aromatic ring to the carbonyl group. Redistribution of intramolecular charges results in internal conversion to the lowest excited singlet state $S_{CT-N}({}^1\pi\pi^*)$. From this state, an intramolecular proton transfer occurs, which triggers decarboxylation. Actually, the ESIPT and decarboxylation processes proceed in an asynchronous concerted way. The ESIPT process is accomplished in the $S_{CT-N}({}^1\pi\pi^*)$ state, but the CO_2 molecule is finally formed in the ground state via the $CI(S_{CT}/S_0)$ conical intersection. In addition, electron transfer and the reverse proton transfer in the ground state play an important role in the formation of the final products. Azomethine ylide is formed in the ground state as a complex with CO_2 , due to



Scheme 2 Mechanistic details for the formation of azomethine ylide by photoreaction of *N*-phthaloylglycine at 266 and 305 nm.

Coulomb interactions. The relatively high barrier on the S_0 pathway to the final product indicates that the azomethine ylide is stable, which is consistent with the experimental findings. This work provides mechanistic details of the formation of azomethine ylide by photoreaction of *N*-phthaloylglycine, which are summarized in Scheme 2. It is to be expected that the formation of azomethine ylide could be a common phenomenon for different types of *N*-phthalimido-amino acids and related compounds, which may stimulate further research interest in the fields of laser spectroscopy and photochemistry.

This work was supported by the National Natural Science Foundation of China (21033002) and the National Basic Research Program of China (2011CB808503)

- 1 Kanaoka Y. Photoreactions of cyclic imides. Examples of synthetic organic photochemistry. *Acc Chem Res*, 1978, 11: 407–413
- 2 Sato Y, Nakai H, Mizoguchi T, Kawanishi M, Hatanaka Y, Kanaoka Y. Photodecarboxylation of *N*-phthaloyl- α -amino acids. *Chem Pharm Bull*, 1982, 30: 1263–1270
- 3 Coyle JD. Phthalimide and its derivatives. In: *Synthetic Organic Photochemistry*. Horspool WM. Ed. Plenum: New York, 1984. 259–284
- 4 Yoon UC, Kim DU, Lee CW, Choi YS, Lee YJ, Ammon HL, Mariano PS. Novel and efficient azomethine ylide forming photoreactions of *N*-(silylmethyl)phthalimides and related acid and alcohol derivatives. *J Am Chem Soc*, 1995, 117: 2698–2710
- 5 Yoon UC, Lee CW, Oh SW, Mariano PS. Exploratory studies probing the intermediacy of azomethine ylides in the photochemistry of *N*-phthaloyl derivatives of α -amino acids and α -amino alcohols. *Tetrahedron*, 1999, 55: 11997–12008
- 6 Formosinho SJ, Arnaut, LG. Excited-state proton transfer reactions II. Intramolecular reactions. *J Photochem Photobiol A Chem*, 1993, 75: 21–48
- 7 Oelgemoller M, Griesbeck AG. Photoinduced electron transfer

- chemistry of phthalimides: An efficient tool for C–C-bond formation. *J Photochem Photobiol C Photochem Rev*, 2002, 3: 109–127
- 8 Yoon UC, Mariano PS. The synthetic potential of phthalimide SET photochemistry. *Acc Chem Res*, 2001, 34: 523–533
- 9 Griesbeck AG, Hoffmann N, Warzecha KD. Photoinduced-electron-transfer chemistry: From studies on PET processes to applications in natural product synthesis. *Acc Chem Res*, 2007, 40: 128–140
- 10 Takahashi Y, Miyashi T, Yoon UC, Oh SW, Mancheno M, Su Z, Falvey DF, Mariano PS. Mechanistic studies of the azomethine ylide-forming photoreactions of *N*-(silylmethyl)phthalimides and *N*-phthaloylglycine. *J Am Chem Soc*, 1999, 121: 3926–3932
- 11 Oelgemoller M, Griesbeck AG, Lex J, Haeuseler A, Schmitt M, Niki M, Hesek D, Inoue Y. Structural, CV and IR spectroscopic evidences for preorientation in PET-active phthalimido carboxylic acids. *Org Lett*, 2001, 3: 1593–1596
- 12 Warzecha KD, Golmer H, Griesbeck AG. Photoinduced decarboxylative benzylation of phthalimide triplets with phenyl acetates: A mechanistic study. *J Phys Chem A*, 2006, 110: 3356–3363
- 13 Soldevilla A, Griesbeck AG. Chiral photocages based on phthalimide photochemistry. *J Am Chem Soc*, 2006, 128: 16472–16473
- 14 Gorner H, Oelgemoller M, Griesbeck AG. Photodecarboxylation study of carboxy-substituted *N*-alkylphthalimides in aqueous solution: Time resolved UV-vis spectroscopy and conductometry. *J Phys Chem A*, 2002, 106: 1458–1464
- 15 Basaric N, Horvat M, Mlinaric-Majerski K, Zimmermann E, Neudorfl J, Griesbeck, AX. Novel 2,4-methanoadamantanebenzazepine by domino photochemistry of *N*-(1-adamantyl)phthalimide. *Org Lett*, 2008, 10: 3965–3968
- 16 Horvat M, Gorner H, Warzecha KD, Neudorfl J, Griesbeck AG, Mlinaric-Majerski K, Basaric N. Photoinitiated domino reactions: *N*-(adamantyl)phthalimides and *N*-(adamantylalkyl)phthalimides. *J Org Chem*, 2009, 74: 8219–8231
- 17 Holmes AB, White JM, Ryan JH. 1,3-Dipolar cycloaddition-decarboxylation reactions of an azomethine ylide with isatoic anhydrides: Formation of novel benzodiazepinones. *Org Lett*, 2011, 13: 486–489
- 18 Andersson K, Barysz M, Bernhardsson A, Blomberg MRA, Carissan Y, Cooper DL, Cossi M, Fleig T, Fülcher MP, Gagliardi L, Graaf CD, Hess BA, Karlström G, Lindh R, Malmqvist PÅ, Neogrády P, Olsen J, Roos BO, Schimmelpfennig B, Schütz M, Seijo L, Serrano-Andrés L, Siegbahn PEM, Ståhring J, Thorsteinsson T, Veryazov V, Wierzbowska M, Widmark PO, Molcas Version 7.1, University of Lund: Sweden, 2008
- 19 Frisch MJ, Trucks GW, Schlegel HB, Scuseria GE, Robb MA, Cheeseman JR, Montgomery Jr. JA, Vreven T, Kudin KN, Burant JC, Millam JM, Iyengar SS, Tomasi J, Barone V, Mennucci B, Cossi M, Scalmani G, Rega N, Petersson GA, Nakatsuji H, Hada M, Ehara M, Toyota K, Fukuda R, Hasegawa J, Ishida M, Nakajima T, Honda Y, Kitao O, Nakai H, Klene M, Li X, Knox JE, Hratchian HP, Cross JB, Adamo C, Jaramillo J, Gomperts R, Stratmann RE, Yazyev O, Austin AJ, Cammi R, Pomelli C, Ochterski JW, Ayala PY, Morokuma K, Voth GA, Salvador P, Dannenberg JJ, Zakrzewski VG, Dapprich S, Daniels AD, Strain MC, Farkas O, Malick DK, Rabuck AD, Raghavachari K, Foresman JB, Ortiz JV, Cui Q, Baboul AG, Clifford S, Cioslowski J, Stefanov BB, Liu G, Liashenko A, Piskorz P, Komaromi I, Martin RL, Fox DJ, Keith T, Al-Laham MA, Peng CY, Nanayakkara A, Challacombe M, Gill PMW, Johnson B, Chen W, Wong MW, González C, Pople JA. Gaussian03 Revision C.02, Gaussian, Inc.: Pittsburgh, PA, 2004
- 20 Chen XB, Fang WH. Insight into photodissociation dynamics of benzamide and formanilide from *ab initio* calculations. *J Am Chem Soc*, 2004, 126: 8976–8980
- 21 Fang WH. *Ab initio* determination of dark structures in radiationless transitions for aromatic carbonyl compounds. *Acc Chem Res*, 2008, 41: 452–458
- 22 Turro NJ. *Modern Molecular Photochemistry*. University Science Books: Sausalito, 1991